



# Nonlinear optical properties of near-infrared region Ag<sub>2</sub>S quantum dots pumped by nanosecond laser pulses

Li-wei Liu<sup>\*1,2</sup>, Si-yi Hu<sup>1,2</sup>, Yin-ping Dou<sup>1</sup>, Tian-hang Liu<sup>1</sup>, Jing-quan Lin<sup>1</sup> and Yue Wang<sup>1,2</sup>

## Full Research Paper

[Open Access](#)

### Address:

<sup>1</sup>School of Science, Changchun University of Science and Technology, Changchun, Jilin, 130022, China and <sup>2</sup>International Joint Research Center for Nanophotonics and Biophotonics, Changchun, Jilin, 130022, China

### Email:

Li-wei Liu\* - liulw@cust.edu.cn

\* Corresponding author

### Keywords:

nonlinear optics; quantum dots; silver sulfide (Ag<sub>2</sub>S); strong absorption

*Beilstein J. Nanotechnol.* **2015**, *6*, 1781–1787.

doi:10.3762/bjnano.6.182

Received: 25 January 2015

Accepted: 17 July 2015

Published: 24 August 2015

Associate Editor: J. J. Schneider

© 2015 Liu et al; licensee Beilstein-Institut.

License and terms: see end of document.

## Abstract

This study investigates near-infrared region Ag<sub>2</sub>S quantum dots (QDs) and their nonlinear optical response under 532 nm nanosecond laser pulses. Our experimental result shows that nonlinear transmission is reduced from 0.084 to 0.04. The observed narrowing behavior of the output pulse width shows superior optical limiting. We discuss the physical mechanisms responsible for the nonlinear optical response of the QDs. The average size of the nanocrystals was 5.5 nm. Our results suggest the possibility of using these Ag<sub>2</sub>S QDs for photoelectric, biosensor, optical ranging, and self-adaptive technologies.

## Introduction

Quantum dots (QDs) are semiconductor nanostructures with a size from 3 to 10 nm [1]. Through tailoring their size and composition, the emission wavelength of the quantum dots can be tuned from 650 to 1250 nm. In the last ten years, the study and development of QDs has rapidly progressed, and also influenced other research areas, such as nonlinear optics, plasmonics and biosensors. The special optical properties of QDs include good resistance to photo-bleaching, large absorption cross section, long fluorescence lifetimes, high quantum yields, and luminescence emission with large Stokes shift [2]. The development of synthetic nanoparticles has facilitated research on the nonlinear behavior of QDs and shown the great potential

of QDs for different applications [3,4]. The synthesis of QDs with nonlinear behavior has been accomplished in aqueous solution over the past two decades [5,6]. Recently, studies have reported on nonlinear optical properties of QDs. Given their potential for various applications, including nonlinear reflectivity, efforts have recently been devoted to identifying QDs with near-infrared region (NIR) emission, such as PbSe, PbS, and CuInS<sub>2</sub> [7,8]. These are non-cadmium-based QDs, and the use of NIR light solves the autofluorescence problem through the reduction of the fluorescence background [9-11]. Previous research has demonstrated that Ag<sub>2</sub>S QDs may be good candidates for use as NIR emitters [12-19]. Ag<sub>2</sub>S QDs have a band

gap of 1.1 eV, the appropriate narrow band gap for NIR emission, and a relatively large absorption coefficient, which may enhance the emission intensity. Therefore, Ag<sub>2</sub>S QDs provide a powerful route for improving the optical properties of semiconductor nanocrystals [20–22]. Ag<sub>2</sub>S QDs have a wide range of applications in optical and other research fields. The development of their synthesis method may facilitate their application in optoelectronic devices for light absorption, photoconductor cells, IR detectors and so on [21,23–28].

Various optical properties of semiconductor or metallic nanoparticles with different sizes and shapes, such as nonlinear absorption and scattering, have been investigated both theoretically and experimentally [29–35]. However, there is a lack of research on the nonlinear properties of laser-pumped NIR QDs. In this study, we report experimental results of nonlinear optical behavior of Ag<sub>2</sub>S QDs pumped by 532 nm nanosecond laser pulses. The results of spectral, spatio-temporal and pump waveform measurements from laser pump energy effect are presented in this study and explained on the basis of the nonlinear optics theory of nanoparticles.

## Results and Discussion

Figure 1 shows the analysis of a sample of Ag<sub>2</sub>S nanocrystals dispersed in chloroform (CHCl<sub>3</sub>). The QDs were synthesized using the typical procedure published previously [20]. The sizes of the QDs were determined using a JEOL JEM-100cx transmission electron microscope (TEM) with an accelerating voltage of 80 kV. The TEM image of Ag<sub>2</sub>S is shown in Figure 1a. The particles are estimated to have an average diameter of 5–6 nm.

Figure 1a shows the absorption spectra of Ag<sub>2</sub>S QDs, measured by a scanning spectrophotometer (UV-3101PC from Shimadzu). Figure 1b shows the EDS spectra of Ag<sub>2</sub>S QDs clearly indicating Ag and S as constituents. The two sharp

peaks at 0 and 0.15 keV have no relation to the Ag<sub>2</sub>S quantum dots, and are caused by a measurement error.

COMSOL Multiphysics 4.2a was used to simulate nonlinear optical characteristics for Ag<sub>2</sub>S QDs. Full-wave 2D analysis with Gaussian laser beam profile was employed. In order to reduce the needed computational resources, the model size was defined as 300 × 2000 nm, and the circles represent the quantum dots, as shown in Figure 2a. The following equations were used to describe the electric field (z-component):

$$E(x, y, z) = E_0 \sqrt{\frac{\omega_0}{\omega(x)} e^{-\left[ \frac{y}{\left( \omega_0 \sqrt{1 + \left( \frac{x}{x_0} \right)^2} \right)^2} \right]^2}} \times \cos \left[ \omega t - kx + \frac{1}{2} \arctan \left( \frac{x}{x_0} \right) - \frac{\kappa y^2}{2x \left( 1 + \left( \frac{x_0}{x} \right)^2 \right)} \right] \vec{e}_z, \quad (1)$$

$$E(x, y, z) = E_0 \sqrt{\frac{\omega_0}{\omega(x)} e^{-\left( \frac{y}{\omega(x)} \right)^2}} \times \cos \left( \omega t - kx + \eta(x) - \frac{\kappa y^2}{2R(x)} \right) \vec{e}_z, \quad (2)$$

where  $\omega_0$  is the minimum waist,  $\omega$  is the angular frequency,  $y$  is the in-plane transverse coordinate, and  $k$  is the wave number. The simulation parameters are shown in Table 1.

The results of simulations are presented in Figure 2b, the dots in the rectangle represent the Ag<sub>2</sub>S QDs. One can see that the Ag<sub>2</sub>S QDs can show nonlinear optical phenomena under 532 nm laser irradiation. The intensity of the electric field changes drastically when the laser passes through the quantum

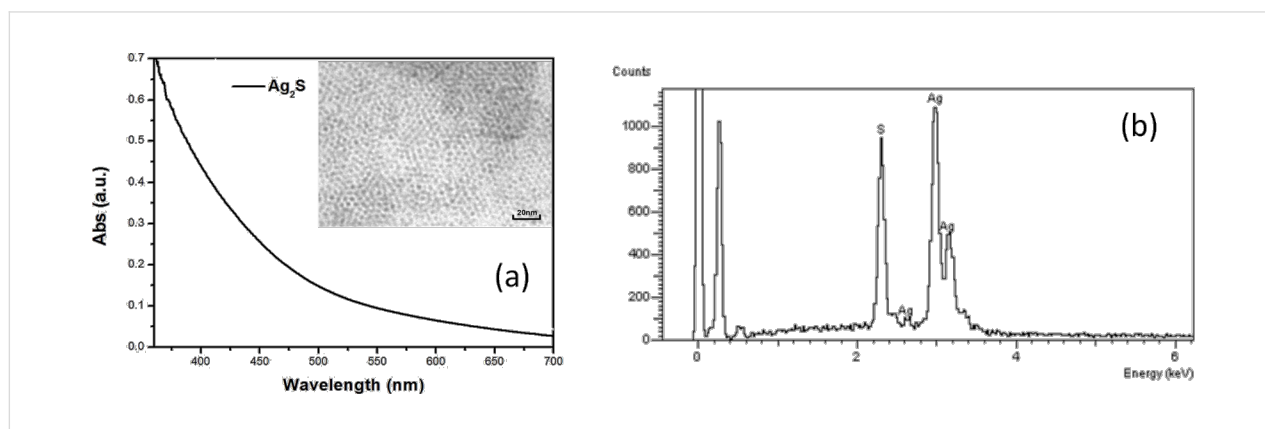


**Figure 1:** (a) Absorption spectra of Ag<sub>2</sub>S QDs in chloroform, the TEM image of Ag<sub>2</sub>S QDs is shown in the inset. (b) EDS spectra of Ag<sub>2</sub>S QDs.

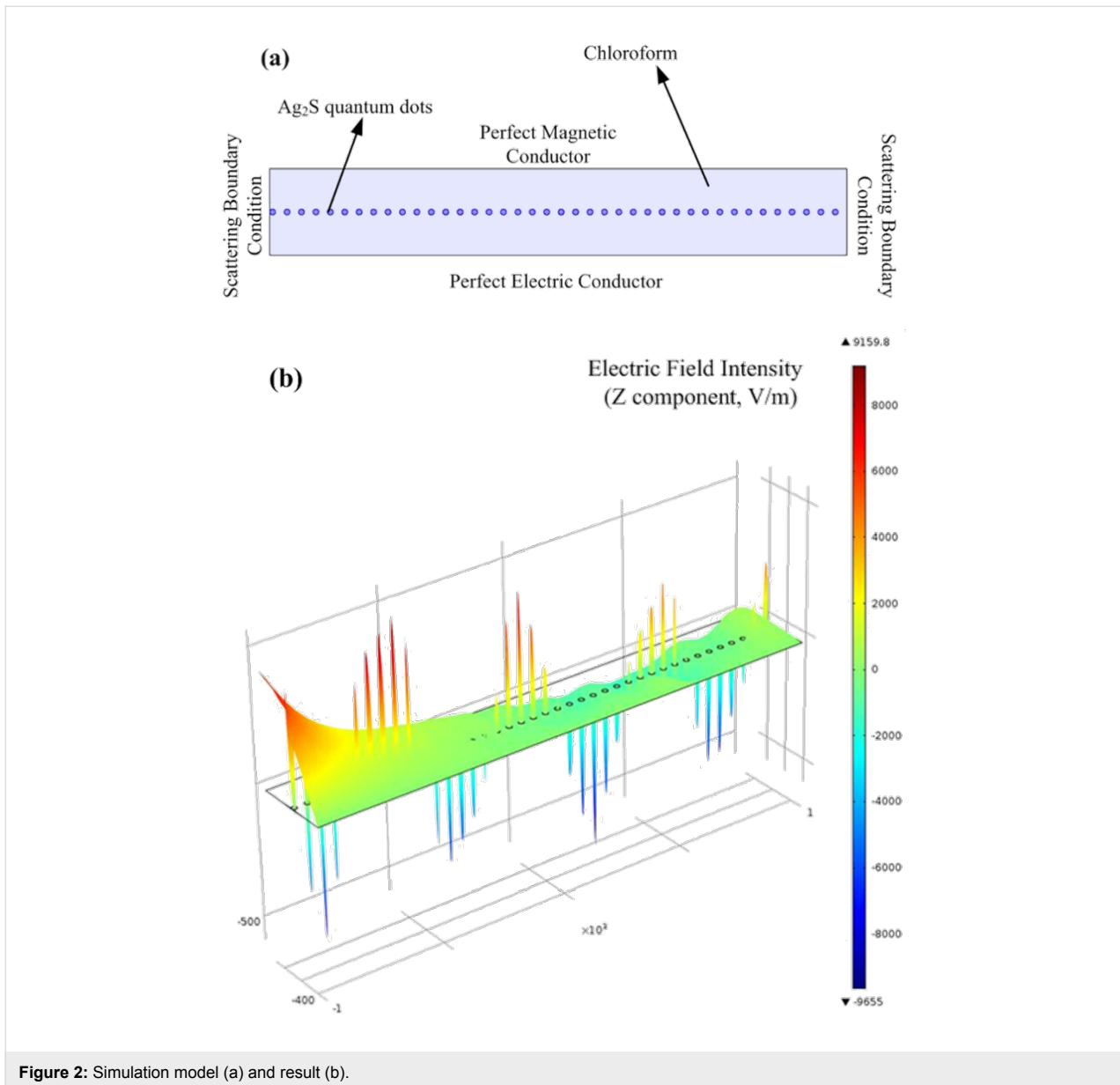


**Figure 2:** Simulation model (a) and result (b).

**Table 1:** Simulation parameters.

name	value	description
$\omega_0$	2 [ $\mu\text{m}$ ]	minimum waist
$\lambda_0$	532 [nm]	laser wavelength
$E_0$	30 [kV/m]	peak electric field
$x_0$	$\pi \cdot \omega_0^2 / \lambda_0$	Rayleigh range
$k_0$	$2\pi / \lambda_0$	propagation constant
$\omega_0$	$k_0 \cdot c$	Angular frequency
$dt$	8.9 [ns]	pulse width

dots. Previous research attributed the nonlinear optical behavior of nanoparticles to the reverse saturable absorption, when the nanoparticle were pumped by nanosecond laser pulses at a

wavelength of 532 nm [36]. When the nanoparticles were pumped by femtosecond or picosecond laser pulses at wavelengths of 800 or 1064 nm, the nanoparticles exhibited self-focusing effects or positive nonlinear absorption, which reduced the nonlinear optical signal of nanoparticles [36-40].

Figure 3 shows the experimental setup. The pump source is a 532 nm Nd:YAG laser with tunable pulse width [41]. The repetition rate was 10 Hz. Input pump pulses were focused with an  $f=5$  cm lens onto the center of a quartz cuvette with the sample solution. The optical path length of the focused pump beam passing through the sample medium was 2 cm, and the minimum waist of the laser is  $3 \pm 1 \mu\text{m}$ , the Rayleigh range of the laser is 53.12  $\mu\text{m}$ .

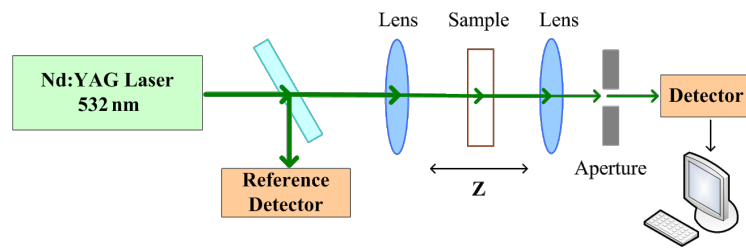


Figure 3: Experimental setup.

Briefly, a Z-scan is one of the commonly utilized methods to measure nonlinear behavior. In this study, we used “open-aperture” and “closed-aperture” experiments according to Ganeev et al. [40]. Moreover, to check for the presence of nonlinear scattering, we used a photodiode placed at a fixed angle of about 40°. Insignificant nonlinear scattering of the laser beam was observed. Figure 4 shows the recorded Z-scan graphs of the Ag<sub>2</sub>S QDs. The laser pump energy ranged from 25 to 45 mJ.

We can see that all the open-aperture Z-scan exhibit a transmission maximum at low laser energy, indicating a saturable absorption behavior. However, there is a dip in the center of the transmission maximum with the laser energy increasing [42]. There is also a transmission minimum at higher laser energy, indicating a reverse saturable absorption behavior [22]. The curves of the closed-aperture Z-scans show different shapes compared to the open-aperture Z-scans, which is because of the combination of nonlinear effects in the system [22]. When the laser interacts with the QDs, free-carrier absorption, nonlinear scattering, and saturable absorption will occur, which all contribute to nonlinear behavior.

In semiconductor QDs the absorption coefficient and cross section were found to be the major properties that are largely affected by the structure of the semiconductor. Table 2 and Table 3 list the fitted nonlinear optical parameter of Ag<sub>2</sub>S QDs for open-aperture Z-scan and closed-aperture Z-scan. The data in the table have an estimated error of 15%, which is caused by the energy fluctuations of the laser beam and air turbulences.

We measured the pulse energy values of the input and the transmitted laser beams to get a larger detecting area compared to the beam cross section. In our case, the dynamic transmission of the sample is determined by [41]:

$$T(I_0) = T_0 T'(I_0) = T_0 \frac{\ln(1 + \beta L I_0)}{\beta L I_0}. \quad (3)$$

Here,  $T_0$  is the linear transmission,  $T'$  is the nonlinear transmission,  $I_0$  is the input pulse energy, and the absorption coefficient  $\beta$  was obtained through Equation 4:

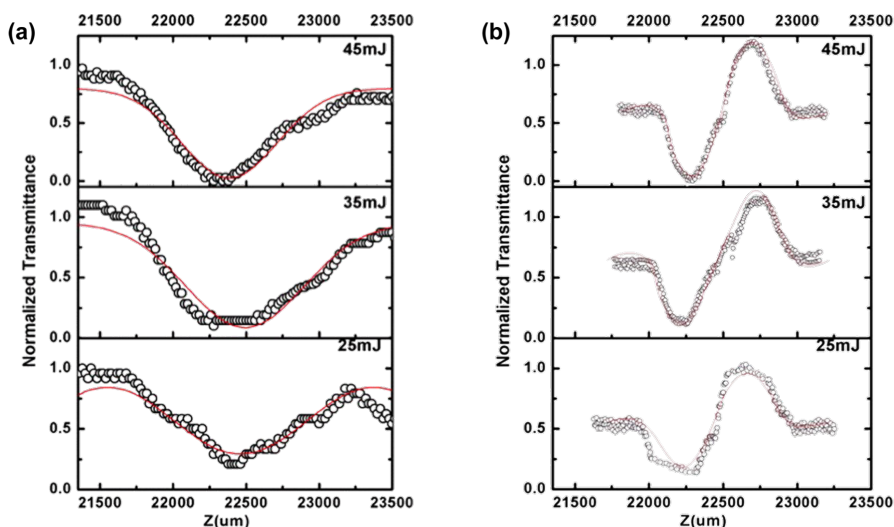


Figure 4: (a) Open-aperture Z-scan graph of Ag<sub>2</sub>S QDs; (b) closed-aperture Z-scan graph of Ag<sub>2</sub>S QDs.

**Table 2:** Fitted nonlinear optical parameter of Ag<sub>2</sub>S QDs for open-aperture Z-scans.<sup>a</sup>

laser energy (mJ)	linear absorption coefficient $\alpha$ (cm <sup>-1</sup> )	estimated size (nm)	absorption coefficient $\beta_2$ ( $\times 10^{-3}$ cm/GW)	cross section $\sigma_2$ ( $\times 10^4$ GW)
25	0.32	5.2	1.889	3.899
35	0.23	5.2	0.686	1.416
45	0.16	5.2	0.376	0.775

<sup>a</sup>All values listed have an estimated error of 15%.**Table 3:** Fitted nonlinear optical parameter of Ag<sub>2</sub>S QDs for closed-aperture Z-scans.<sup>a</sup>

laser energy (mJ)	linear absorption coefficient $\alpha$ (cm <sup>-1</sup> )	estimated size (nm)	absorption coefficient $\beta_2$ ( $\times 10^{-3}$ cm/GW)	cross section $\sigma_2$ ( $\times 10^4$ GW)
25	0.32	5.2	1.193	2.462
35	0.23	5.2	0.305	0.629
45	0.16	5.2	0.095	0.195

<sup>a</sup>All values listed have an estimated error of 15%.

$$\beta = 2^{3/2} \cdot \frac{(1-T_0)}{\left(\frac{2P}{\pi\omega_0^2 \cdot L_{\text{eff}}}\right)} \quad (4)$$

Here,  $T_0$  is the normalized peak height,  $P$  is the pulse peak power,  $\omega_0$  is the beam waist radius,  $L_{\text{eff}}$  is the effective length in medium. The cross section  $\sigma$  was obtained by Equation 5:

$$\sigma_2 = \frac{10^3 \beta_2 h\nu}{N_0 C} \quad (5)$$

Here,  $C$  is concentration,  $h\nu$  is the energy of incident light,  $N_0$  is a molecular number of quantum dots solutions. We set  $L$  as the constant optical path in the sample. As shown in Figure 5 we can see that the measured nonlinear transmission value is reduced from 0.084 to 0.04 when the input pulse energy increased. Figure 6a shows the waveforms of pulse and transmission pulse measured at the same pump energy level (40 mJ) by a two-channel digital oscilloscope of 200 MHz bandwidth (TDS 2024B).

It can be seen that the laser pulse width is 22.8 ns for a pump energy of 40 mJ. The transmission pulse is 10.5 ns for Ag<sub>2</sub>S QDs, and 21.08 ns for CHCl<sub>3</sub>. The transmission pulse of nanostructure particles is much shorter than that of the laser pulse. Figure 6b shows the transmission pulses at a different pump energy level. The waveforms became narrower as the laser pump energy increased. In a two-level system, such as this, when the laser pulse width is much larger than the particle

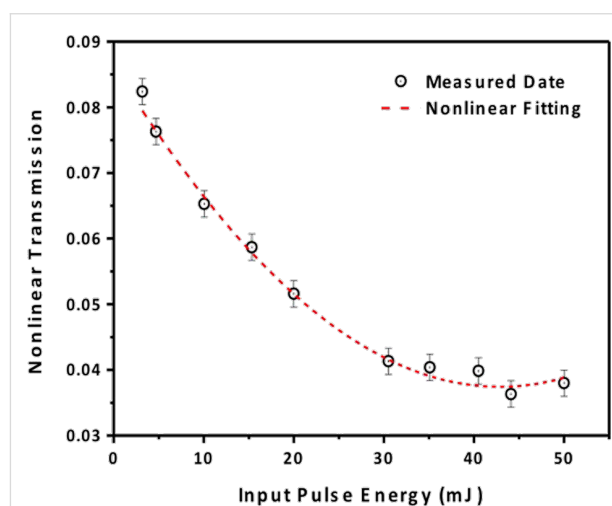


**Figure 5:** Measured nonlinear transmission versus the input pulse energy for Ag<sub>2</sub>S QDs. The dashed line represents the best fitting curve based on Equation 3 with  $\beta = \text{constant}$ .

relaxation time, multiple absorption will occur in the QDs. For Ag<sub>2</sub>S QDs, a large Ag protrusion is formed in the nanogap when the laser pump energy increased. Both electronic and ionic currents contribute to the absorption of the Ag<sub>2</sub>S QDs, which is affected by the pulse width waveforms. It could also be explained by an effect of nonlinear optical absorption that depends on the pump energy. This may reflect the dynamic behavior of gain or feedback mechanisms in the nonlinear absorption behavior of nanostructure particles. To exclude the possibility of a nonlinear behavior of nanocrystalline materials, we conducted the experiment for Ag<sub>2</sub>S QDs absorption measurement.

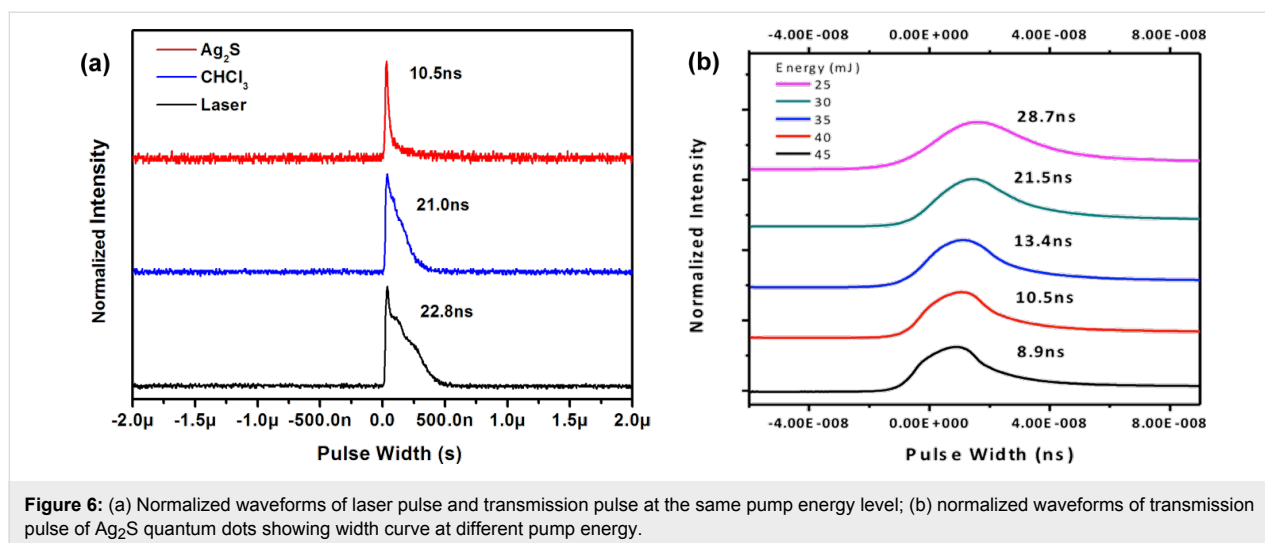


**Figure 6:** (a) Normalized waveforms of laser pulse and transmission pulse at the same pump energy level; (b) normalized waveforms of transmission pulse of Ag<sub>2</sub>S quantum dots showing width curve at different pump energy.

Figure 7 shows the output energy as a function of the input pump energy at different concentration values. The intensity of the absorption is defined as the ratio of the output energy to the input pump energy. It is shown that at the different pump levels, the Ag<sub>2</sub>S sample with a higher concentration (4.0 mg/mL) produced a smaller output energy than the Ag<sub>2</sub>S sample with a lower concentration (2.0 mg/mL). CHCl<sub>3</sub> produced the lowest absorption intensity. Ag<sub>2</sub>S exhibited stronger absorption compared with CHCl<sub>3</sub> as the pump energy increased. This can be explained by the fact that there are many impurities and electron–hole pairs in QDs. Also, when the laser interacts with QDs the dielectric constant of the medium surrounding the QDs will be changed. Ag<sub>2</sub>S has a narrow band gap, which leads to the strong absorption characteristics of Ag<sub>2</sub>S and which makes Ag<sub>2</sub>S particularly suitable for use in optical detectors and solar cells.

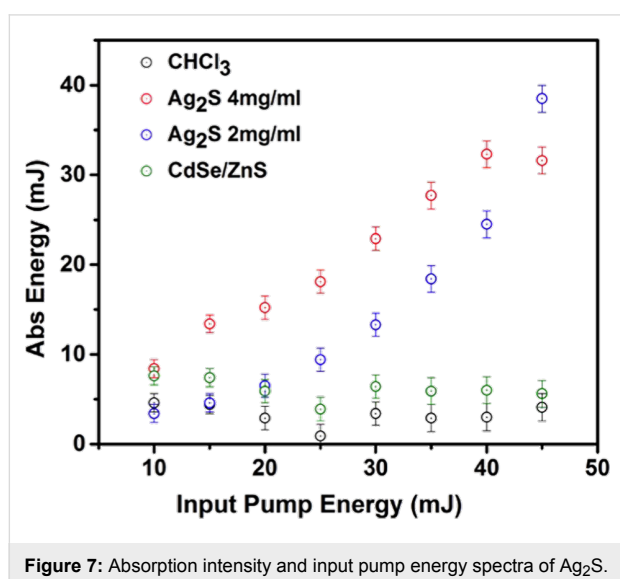


**Figure 7:** Absorption intensity and input pump energy spectra of Ag<sub>2</sub>S.

## Conclusion

In summary, we have demonstrated, using NIR Ag<sub>2</sub>S QDs pumped by 532 nm nanosecond pulses, that the nonlinear optical characteristics can be efficiently generated in QDs. The simulation results show the nonlinear characteristics of Ag<sub>2</sub>S QDs. Nonlinear transmission measurement revealed that Ag<sub>2</sub>S QDs have a superior nonlinear optical performance because of their strong absorption characteristics, and can compress pump pulse waveform. The strong absorption characteristics of Ag<sub>2</sub>S QDs may lead to more uses for nonlinear applications. This makes them promising candidates for nonlinear optical studies and the potential future applications of nanoparticles. We also note that in future research we may explore further the specific physical mechanisms and dynamics of nanoparticles with laser technology.

## Acknowledgements

This work was supported by the National Natural Science Foundation of China (No. 11204020).

## References

- Prasad, P. N. *Nanophotonics*; Wiley-Interscience: New York, NY, U.S.A., 2004. doi:10.1002/0471670251
- Liu, L.; Hu, R.; Law, W.-C.; Roy, I.; Zhu, J.; Ye, L.; Hu, S.; Zhang, X.; Yong, K.-T. *Analyst* **2013**, *138*, 6144–6153. doi:10.1039/c3an01030a
- Kim, K. S.; Hur, W.; Park, S.-J.; Hong, S. W.; Choi, J. E.; Goh, E. J.; Yoon, S. K.; Hahn, S. K. *ACS Nano* **2010**, *4*, 3005–3014. doi:10.1021/nn100589y
- Vivas, M. G.; Cury, J. F.; Schiavon, M. A.; Mendonca, C. R. *J. Phys. Chem. C* **2013**, *117*, 8530–8535. doi:10.1021/jp400956k
- Bothun, G. D.; Rabideau, A. E.; Stoner, M. A. *J. Phys. Chem. B* **2009**, *113*, 7725–7728. doi:10.1021/jp9017458
- Rivera Gil, P.; Parak, W. J. *ACS Nano* **2008**, *2*, 2200–2205. doi:10.1021/nn800716j
- Wehrenberg, B. L.; Wang, C.; Guyot-Sionnest, P. *J. Phys. Chem. B* **2002**, *106*, 10634–10640. doi:10.1021/jp021187e

8. Bakueva, L.; Gorelikov, I.; Musikhin, S.; Zhao, X. S.; Sargent, E. H.; Kumacheva, E. *Adv. Mater.* **2004**, *16*, 926–929. doi:10.1002/adma.200306458
9. Kim, S.; Lim, Y. T.; Soltész, E. G.; De Grand, A. M.; Lee, J.; Nakayama, A.; Parker, J. A.; Mihaljevic, T.; Laurence, R. G.; Dor, D. M.; Cohn, L. H.; Bawendi, M. G.; Frangioni, J. V. *Nat. Biotechnol.* **2004**, *22*, 93–97. doi:10.1038/nbt920
10. Balet, L. P.; Ivanov, S. A.; Piryatinski, A.; Achermann, M.; Klimov, V. I. *Nano Lett.* **2004**, *4*, 1485–1488. doi:10.1021/nl049146c
11. Blackman, B.; Battaglia, D.; Peng, X. *Chem. Mater.* **2008**, *20*, 4847–4853. doi:10.1021/cm8000688
12. Liu, Z.; Tabakman, S.; Sherlock, S.; Li, X.; Chen, Z.; Jiang, K.; Fan, S.; Dai, H. *Nano Res.* **2010**, *3*, 222–233. doi:10.1007/s12274-010-1025-1
13. Smith, A. M.; Mancini, M. C.; Nie, S. *Nat. Nanotechnol.* **2009**, *4*, 710–711. doi:10.1038/nnano.2009.326
14. Masuo, S.; Naiki, H.; Machida, S.; Itaya, A. *Appl. Phys. Lett.* **2009**, *95*, 193106. doi:10.1063/1.3259792
15. Yeh, Y.-C.; Yuan, C.-T.; Kang, C.-C.; Chou, P.-T.; Tang, J. *Appl. Phys. Lett.* **2008**, *93*, 223110. doi:10.1063/1.3021366
16. Yuan, C. T.; Chou, W. C.; Chuu, D. S.; Chen, Y. N.; Lin, C. A.; Chang, W. H. *Appl. Phys. Lett.* **2008**, *92*, 183108. doi:10.1063/1.2921779
17. Allen, P. M.; Bawendi, M. G. *J. Am. Chem. Soc.* **2008**, *130*, 9240. doi:10.1021/ja8036349
18. Welsher, K.; Liu, Z.; Sherlock, S. P.; Robinson, J. T.; Chen, Z.; Daranciang, D.; Dai, H. *Nat. Nanotechnol.* **2009**, *4*, 773–780. doi:10.1038/nnano.2009.294
19. Welsher, K.; Sherlock, S. P.; Dai, H. *J. Proc. Natl. Acad. Sci. U. S. A.* **2011**, *108*, 8943–8948. doi:10.1073/pnas.1014501108
20. Du, Y.; Xu, B.; Fu, T.; Cai, M.; Li, F.; Zhang, Y.; Wang, Q. *J. Am. Chem. Soc.* **2010**, *132*, 1470. doi:10.1021/ja909490r
21. Peng, P.; Sadtler, B.; Alivisatos, A. P.; Saykally, R. J. *J. Phys. Chem. C* **2010**, *114*, 5879–5885. doi:10.1021/jp9116722
22. Liaros, N.; Aloukos, P.; Kolokithas-Ntoukas, A.; Bakandritsos, A.; Szabo, T.; Zboril, R.; Couris, S. *J. Phys. Chem. C* **2013**, *117*, 6842–6850. doi:10.1021/jp400559q
23. Terabe, K.; Hasegawa, T.; Nakayama, T.; Aono, M. *Nature* **2005**, *433*, 47–50. doi:10.1038/nature03190
24. Gao, F.; Lu, Q.; Zhao, D. *Nano Lett.* **2003**, *3*, 85–88. doi:10.1021/nl025811a
25. Huxter, V. M.; Mirkovic, T.; Nair, P. S.; Scholes, G. D. *Adv. Mater.* **2008**, *20*, 2439. doi:10.1002/adma.200702429
26. Lou, W.; Wang, X.; Chen, M.; Liu, W.; Hao, J. *Nanotechnology* **2008**, *19*, 225607. doi:10.1088/0957-4484/19/22/225607
27. Xiang, J.; Cao, H.; Wu, Q.; Zhang, S.; Zhang, X.; Watt, A. A. R. *J. Phys. Chem. C* **2008**, *112*, 3580–3584. doi:10.1021/jp710597j
28. Hirsch, M. P. *Environ. Toxicol. Chem.* **1998**, *17*, 601–604. doi:10.1002/etc.5620170411
29. Lee, K.-S.; El-Sayed, M. A. *J. Phys. Chem. B* **2005**, *109*, 20331–20338. doi:10.1021/jp054385p
30. Jain, P. K.; Lee, K. S.; El-Sayed, I. H.; El-Sayed, M. A. *J. Phys. Chem. B* **2006**, *110*, 7238–7248. doi:10.1021/jp057170o
31. Aslan, K.; Holley, P.; Davies, L.; Lakowicz, J. R.; Geddes, C. D. *J. Am. Chem. Soc.* **2005**, *127*, 12115–12121. doi:10.1021/ja052739k
32. Evanoff, D. D., Jr.; Chumanov, G. *J. Phys. Chem. B* **2004**, *108*, 13957–13962. doi:10.1021/jp0475640
33. Bogatyrev, V. A.; Dykman, L. A.; Khlebtsov, B. N.; Khlebtsov, N. G. *Opt. Spectrosc.* **2004**, *96*, 128–135. doi:10.1134/1.1643997
34. Yguerabide, J.; Yguerabide, E. E. *Anal. Biochem.* **1998**, *262*, 137–156. doi:10.1006/abio.1998.2759
35. He, G. S.; Zhu, J.; Yong, K.-T.; Baev, A.; Cai, H.-X.; Hu, R.; Cui, Y.; Zhang, X.-H.; Prasad, P. N. *J. Phys. Chem. C* **2010**, *114*, 2853–2860. doi:10.1021/jp907811g
36. Fan, G.; Qu, S.; Wang, Q.; Zhao, C.; Zhang, L.; Li, Z. *J. Appl. Phys.* **2011**, *109*, 023102. doi:10.1063/1.3533738
37. Zeng, H.; Yang, Y.; Jiang, X.; Chen, G.; Qiu, J.; Gan, F. *J. Cryst. Growth* **2005**, *280*, 516–520. doi:10.1016/j.jcrysgro.2005.04.004
38. Ganeev, R. A.; Boltaev, G. S.; Tugushev, R. I.; Usmanov, T. *Appl. Phys. B* **2010**, *100*, 571–576. doi:10.1007/s00340-010-3979-9
39. Ganeev, R. A.; Rysanyansky, A. I.; Stepanov, A. L.; Usmanov, T. *Opt. Quantum Electron.* **2004**, *36*, 949–960. doi:10.1007/s11082-004-3392-x
40. Ganeev, R. A.; Suzuki, M.; Baba, M.; Ichihara, M.; Kuroda, H. *J. Appl. Phys.* **2008**, *103*, 063102. doi:10.1063/1.2887990
41. He, G. S.; Oh, H. S.; Prasad, P. N. *Opt. Lett.* **2011**, *36*, 4431–4433. doi:10.1364/OL.36.004431
42. Neo, M. S.; Venkatram, N.; Li, G. S.; Chin, W. S.; Ji, W. *J. Phys. Chem. C* **2010**, *114*, 18037–18044. doi:10.1021/jp104311j

## License and Terms

This is an Open Access article under the terms of the Creative Commons Attribution License (<http://creativecommons.org/licenses/by/2.0>), which permits unrestricted use, distribution, and reproduction in any medium, provided the original work is properly cited.

The license is subject to the *Beilstein Journal of Nanotechnology* terms and conditions: (<http://www.beilstein-journals.org/bjnano>)

The definitive version of this article is the electronic one which can be found at:  
[doi:10.3762/bjnano.6.182](https://doi.org/10.3762/bjnano.6.182)